

Imperial College London
Department of Computing

Automatic Cell Tracking in Noisy Images for Microscopic Image Analysis

Pedro Damian Kostelec

September 2014

Supervised by Ben Glocker

Submitted in part fulfilment of the requirements for the degree of
Master of Science in Computing (Artificial Intelligence) of Imperial
College London

Abstract

Acknowledgement

I offer my sincerest gratitude to life,

The copyright of this thesis rests with the author and is made available under a Creative Commons Attribution Non-Commercial No Derivatives licence. Researchers are free to copy, distribute or transmit the thesis on the condition that they attribute it, that they do not use it for commercial purposes and that they do not alter, transform or build upon it. For any reuse or redistribution, researchers must make clear to others the licence terms of this work.



Contents

1	Introduction	DRAFT I	7
1.1	Motivation	DRAFT I	7
1.2	Objectives	DRAFT I	8
1.3	Contributions	DRAFT I	9
1.4	Thesis structure	DRAFT I	9
2	Related work	NEW	11
2.1	Cell detection	NEW	11
2.2	Cell tracking	NEW	11
2.2.1	Tracking by detection	NEW	11
2.2.2	Tracking by model evolution	NEW	11
2.2.3	Tracking by global data association	NEW	11
3	Detection of cells	NEW	12
3.1	Overview	NEW	12
3.2	Learning to detect non-overlapping cells	NEW	12
3.2.1	Extremal regions	NEW	12
3.2.2	The non-overlap constraint	NEW	12
3.2.3	Formulation of the model	NEW	13
3.2.4	Learning the model	NEW	13
3.2.5	Implementation details	NEW	13
3.2.6	Summary	NEW	13
3.3	Speeding up the algorithm	NEW	13
3.4	Feature selection	NEW	14

4	Tracking of cells	DRAFT I	17
4.1	Cell tracking overview	DRAFT I	17
4.2	Joining cell detections into robust tracklets	DRAFT I	19
4.3	Global data association	DRAFT I	21
4.4	Implementation using linear programming	DRAFT I	23
4.5	Hypotheses likelihood definitions	DRAFT I	24
4.6	Computing the likelihoods	DRAFT I	26
4.7	Features for the linking classifier	OUTLINE	29
4.7.1	Estimating the velocity with Kalman filters	NEW	31
4.7.2	Gaussian broadening feature	DRAFT I	31
4.7.3	Best feature selection	NEW	32
5	Quantitative measurements of cell behaviour	NEW	33
6	Data acquisition and annotation	NEW	34
6.0.4	Cell culture conditions and imaging modality	NEW	34
6.0.5	The annotation tool	NEW	35
6.0.6	Annotating cell images	NEW	35
7	Experimental results	NEW	37
7.1	Cell detector	NEW	37
7.1.1	Performance	NEW	37
7.1.2	Detection accuracy	NEW	37
7.2	Cell tracker	NEW	37
7.2.1	Performance metrics	NEW	39
7.2.2	Performance	NEW	39
7.2.3	Tracking accuracy		39
8	Discussion and conclusion	NEW	40
8.1	Future work	NEW	40
	Bibliography		41

1 Introduction DRAFT I

1.1 Motivation DRAFT I

To develop methods for cell tracking

Recent advances in intravital microscopy enable us to study the behaviour of different cells without excessively modifying the natural environment in which these cells are found within the body of mice.

Neutrophils are a type of leukocytes that have a crucial role in the clearance of infections. A significant reduction in the number of neutrophils in the human body (or in mice) leads to severe immunodeficiency or death.

They can be found in the bone marrow, liver, spleen and lung. Direct observation of neutrophils should help explain their presence in these organs, especially their large quantity in the lung.

A recent study has shown that the lifespan of neutrophils is much longer than previously known (up to 12.5 hours for mice and 5.4 days for humans). Although this specific study is a source of doubtful criticism (cite), the longevity of neutrophils increases during inflammation. This longer lifespan may permit them to perform a wider range of complex activities, beyond the clearance of infections. An analysis of their behaviour as observed through intravital microscopy could help reveal more of their roles.

Finally, there is accumulating evidence to support the existence of different lineages of neutrophils with discrete roles. It is unknown whether these are actually distinct lineages or if they instead all develop from the same neutrophil predecessor.

The observation of neutrophils required the analysis of thousands of frames of microscopy image sequences. The manual annotation of these image sequences in order to extract trajectories of movement of neutrophils is a time consuming and error prone process. Manual annotation severely limits the number of data that can be analysed and slows down the advancement of cell research. It would be a major advance to be able to reliably automatically identify and track cells over time in sometimes noisy complex images.

1.2 Objectives DRAFT I

Neutrophil image sequences obtained *in vivo* are sometimes of low contrast. *In vivo* observation of these cells in the lung is especially difficult due to the motion artefacts. The motion of the lung can also cause the images to fall out of focus, which causes the cells to appear blurred and become difficult to identify and segment.

The aim of this research is to develop methods for cell detection and tracking. This system should be able to accept an image sequences of cells in tissue, identify the cells and track them over the entire sequence.

The identification of cells should take into account the nature of the imaging technique and the quality of obtained images. Simple methods such as thresholding would be too unreliable; more advanced methods need to be investigated.

Also the tracking of cells should take into account the nature of input data. Basic frame-by-frame tracking of cells is likely to have poor results because the cells frequently disappear into the depths of tissue or loose focus. Methods that take into account the temporal behaviour of cells are likely to result in more robust tracking.

Finally, a basic system to compute statistics of the trajectories should be implemented. The system should provide measure of the length of trajectories and different quantifications of their behaviour.

1.3 Contributions DRAFT I

To the best knowledge of the author, this research presents a novel approach to the problem of cell tracking detections that is directly based on the observed data.

The cell tracker module uses a global data association approach to reliably generate cell detection trajectories based on a global decision. This research has upgraded previous methods to rely on a large set of features obtained from observed data. A machine learning approach is used to compute likelihood for linking cell detections into ever longer trajectories. Because the likelihoods are directly obtained from training examples, the method is able to reliably work on noisy datasets, where several frames in a sequence can come out of focus, cells disappear and reappear over time, etc.

A robust pipeline for detection and tracking consisting of a machine learning approach to cells detections from [4], and the data based tracker allows the efficient tracking of cells in difficult imaging conditions.

Finally, an image annotation tool is developed that allows simple dot annotation of cells and linking of cells among frames to represent distinct trajectories.

1.4 Thesis structure DRAFT I

The rest of the thesis is structured as follows.

Chapter 2 is a brief literature survey outlining existing methods for cell detections and tracking.

Chapter 3 describes in more depth how the cell detection module works.

Chapter 4 describes in details the cell tracking module.

Chapter 5 briefly describes the biological statistics module, which quantifies the obtained cell trajectories.

Chapter 6 is an overview of the cell annotation tool developed to ease the annotation of image sequences.

Chapter 7 evaluates the performance of the cell tracking module.

Chapter 8 shows some concluding remarks and ideas that could be implemented to continue the advance the field of automatic cell detection and tracking.

2 Related work NEW

2.1 Cell detection NEW

2.2 Cell tracking NEW

2.2.1 Tracking by detection NEW

2.2.2 Tracking by model evolution NEW

2.2.3 Tracking by global data association NEW

Rewrite the literature survey to be more concise and to the point

Summarize the difference approaches
- frame to frame,
global

3 Detection of cells NEW

3.1 Overview NEW

what it does

that it learns from datasets which is required to make it robust in noisy datasets

that it is mostly Arteta's work, with some modifications to make it run faster

3.2 Learning to detect non-overlapping cells NEW

Check both Arteta's papers on the subject

Subsection with the changes that were made to Arteta's work

Rewrite: Several of these subsections are directly taken from Arteta's paper. They are meant as guidance, but should be adapted appropriately.

3.2.1 Extremal regions NEW

what are extremal regions and that they are obtained from the MSER feature detector

why are they good: fast, robust to contrast and to what else

what is their work in the detector: they are candidate cells, that are then evaluated as cell/no-cell

3.2.2 The non-overlap constraint NEW

What it means: we can't detect overlapping cells

why is that ok: the datasets don't exhibit such behavior. much more training data would be required, which means more annotations.

3.2.3 Formulation of the model NEW

???

3.2.4 Learning the model NEW

Info about the binary/structural classifier

3.2.5 Implementation details NEW

Dynamic programming for inference NEW

3.2.6 Summary NEW

3.3 Speeding up the algorithm NEW

review this section

The main drawback of the algorithm presented by Arteta [4] is the poor performance. The original algorithm took about 30 seconds to detect cells in a 400x400 image. Because we will be processing hours of microscopy video it was important to reduce the detection time as much as possible. The major performance improvements were achieved by addressing three things.

The algorithm needs to extract a set of features on every single detected MSER. First, we have first fine-tuned the MSER detector to detect less cells, more robustly.

Second, we have identified features that are slow to compute and improved their algorithmic behaviour. One such feature is the Contour Points Distribution Histogram implemented in *cpdh.m*. The function was performing excessive calls to slow functions to extract region characteristics, and was rewritten to call these functions less often, without

affecting its value.

Second, several MATLAB builtin function were modified to remove excessive parameter checking, which in several cases represented an overhead of over 30%. These parameter checks are welcome when developing the algorithm, but once the algorithm is complete, several of these checks can be safely removed.

These optimizations resulted in a significant performance boost. Instead of 30 seconds, the algorithm can now detect cells on the same images in about .

Rewrite: Not sure
I can write this,
since the mat-
lab code is copy-
righted

3.4 Feature selection NEW

The effectiveness of the machine learning method to detect cells depends on the quality of features. Good features have a lot of discriminative power between cells and non cells. The used approach classifies extremal regions as cell/non-cell. The regions are extracted using the MSER detector. Then each region is processed and features are extracted from it. We have evaluated several combinations of these features:

Measure the num-
ber of seconds
it takes to pro-
cess one of these
400x400 images

1. the area A of the region represented by a 10-dimensional binary vector with the entry $\lceil \log A \rceil$ set to 1.
2. 10-dimensional histogram of intensities within the region
3. the position of the descriptor in the image in terms of x-y coordinates of a centroid fitted to the descriptor.
4. two 6-dimensional histograms of differences in intensities between the region border and a dilation of it for two different dilation radii
5. a shape descriptor represented by a 60-dimensioal histogram of the distribution of the boundary of the region on a size-normalized polar coordinate system

6. The orientation of the descriptor after attempting to normalize its orientation
7. The proportion of edge-pixels in the region.

Each of these features has different discriminative power, and takes some time to compute. The application of the cell detector requires that images are processed within a time limit. For this reason, we have trained and tested the algorithm with all the $2^7 - 1$ possible combinations of these features.

We have also developed a function that helps select the most appropriate set of features given specific constraints, for example a maximum computation time, minimal precision and recall values, etc. A graph generated by the function is shown in figure 3.1.

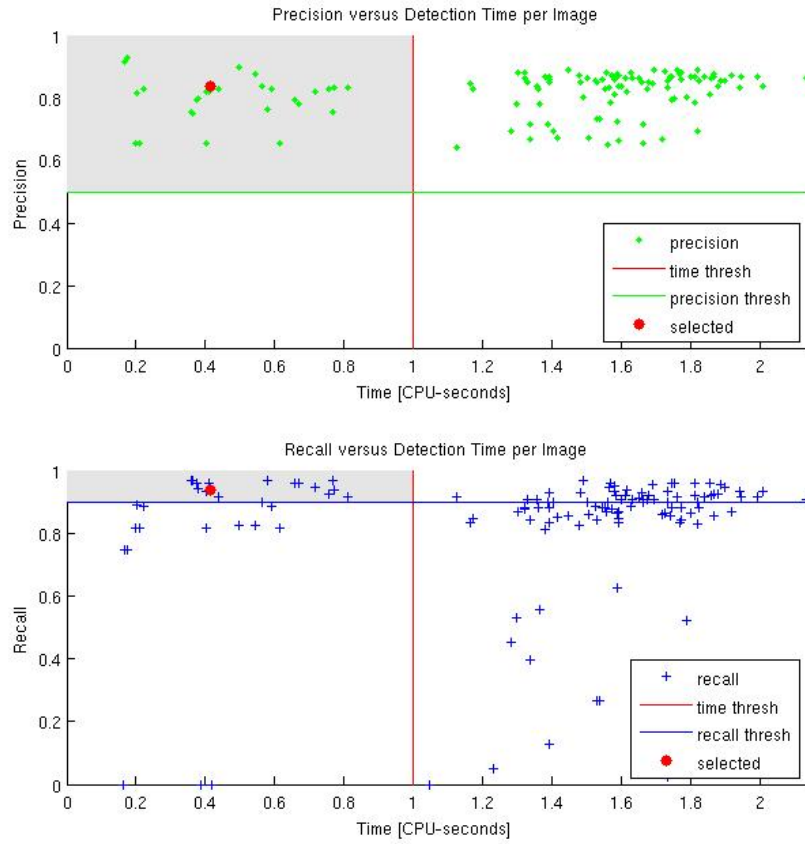


Figure 3.1: The plots helps the user to select the most appropriate feature, given a combination of computation time per image, mean precision and recall. This example, which was obtained by selecting only within feature sets that compute in less than 1 CPU-second, have at least 0.5 precision and 0.9 recall have resulteds in a feature set containing features 1, 3 and 4. Most importance was given to precision followed by computation time and recall. The selected feature set computes in 0.414 cpu-seconds (Intel(R) Core(TM) i7-2600 CPU @ 3.40GHz) per image, with mean precision of 0.836 and mean recall of 0.9363.

4 Tracking of cells DRAFT I

4.1 Cell tracking overview DRAFT I

The cell detections obtained using the method described in chapter 3 need to be linked into trajectories. The detections contain a number of false positives and false negatives (missed detections) which make the task of associating them into trajectories difficult.

First, we define the terminology used in the subsequent sections. A robust tracklet is sequence of cell detections that can be linked with high confidence. These are likely to be detections that are distant from other detections and that were segmented with high accuracy, such that their feature vectors are very similar. A robust tracklet cannot have gaps (missing detections). Similarly a tracklet is a sequence of cell detections, but differ from robust tracklets by the fact that it can contain gaps (missed detections). A sequence of one or more robust tracklets is a tracklet, but the opposite is not always true. Finally, we call a trajectory a sequence of tracklets that can not be effectively linked to any other tracklets. A trajectory is a maximally linked tracklet, and corresponds to the actual path performed by a cell in the image sequence.

Linking cell detections into tracklets is performed in two steps, as seem in fig. 4.1. First, cell detections are linked into robust tracklets by a reliable linking model. Second, the tracklets are iteratively associated into ever longer tracklets by closing ever larger gaps. A detailed overview of these two steps is provided in the remaining of the chapter.

Make sure to update this if no longer iterative

The process of linking robust tracklets into trajectories is performed globally, by selecting the optimal subset of tracklets to link in each

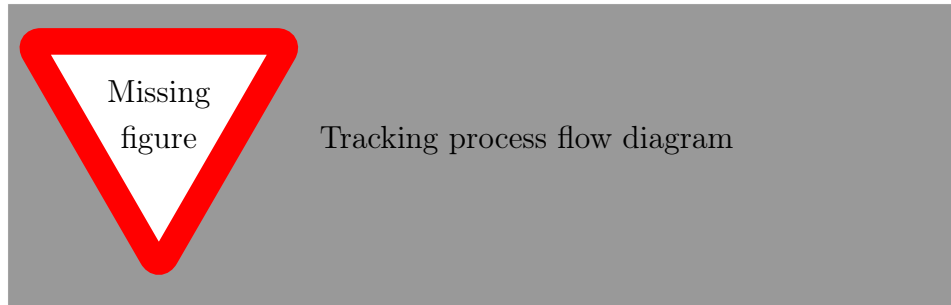


Figure 4.1: Some caption

iteration. This global data association approach has been chosen because it has shown significant improvements in tracking performance compared to other models.

The approach used in this project is similar to [5] in the formulation of the maximum a posteriori probability (MAP) problem and solving it using linear programming, but the hypothesis' likelihoods (the likelihood of linking two tracklets, the likelihood of a tracklet being the first tracklet in a trajectory, the likelihood of it being the last tracklet in a trajectory or the likelihood of it being a false positive) were computed using a machine learning approach. This approach makes it possible to associate cells in very noisy and low quality images, where accurate cell detections are not always possible.

Although the developed system is fully automatic, it gives some control to the user by letting him tweak the hypothesis' likelihoods and thus change the way the tracklets are linked. This control eliminates the need to retrain a specific model for each new dataset, as it makes it possible to use a trained linking model to link robust tracklets in a slightly different and previously unseen dataset.

(level sets [the IMM paper from bise/kanade]) Add references about global data optim better that level sets/frame by frame assoc

4.2 Joining cell detections into robust tracklets DRAFT I

The first phase of linking cell detections into trajectories consists of identifying a set of robust tracklets. An example dataset with the identified robust tracklets is shown in fig. 4.2

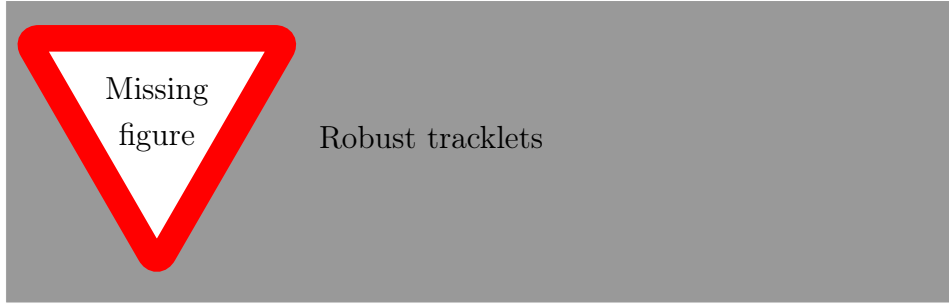


Figure 4.2: Robust tracklets

We define a cell detection $d_i = (x_i, y_i, f_i, t_i)$, where x_i and y_i are the position of the cell detections within the frame, f_i an appearance feature vector obtained from the cell detector module, and t_i the frame index of the detection. The set of all cell detections in the image sequence is $\mathbf{D} = \{d_i\}$.

Define cell detection in the detection chapter

Let $\mathbf{T} = \{T_k\}$ be a hypothesis set of tracklets, where each tracklet is defined as a list of robust tracklets, such that the frame index of the last detection ($t_{k_{in}}$) in each robust tracklets is lower than the frame index of the first detection of any following tracklet ($t_{k_{i+1_1}}$): $T_k = \{T_k^{robust} | \forall i, t_{k_{in}} < t_{k_{i+1_1}}\}$. A robust tracklet is defined as $T_k^{robust} = \{d_{k_i} | \forall i, t_{k_{i+1}} = t_{k_i} + 1, d_{k_i} \in \mathbf{D}\}$. Assuming that each detection can belong to only one tracklet we define the non-overlap constraint:

$$\forall T_i, T_j \in \mathbf{T}, i \neq j, T_i \cap T_j = \emptyset$$

For each cell detection we need to identify a good match in the next

add some words about the feature vector – which features

frame, if it exists. Let P_{link} represent the a likelihood of linking two detections d_i to d_j :

$$P_{link}(d_j|d_i) = \begin{cases} V((f_i, x_i, y_i), (f_j, x_j, y_j)) & \text{if } t_j - t_i = 1 \\ 0 & \text{otherwise} \end{cases},$$

where V is an affinity function that returns the probability that the provided feature vectors and detection positions belong to the same cell.

The probability of linking detections P_{link} is computed on all pairs of cells between consecutive frames i and $i+1$ and vice versa. For each cell detection in the first frame we found the most similar detection in the next frame, and for each detection in the second frame the most similar detection in the previous frame. Then, only symmetrical matches were chosen. A matching is symmetric if a detection in the first frame d_1 best matches detection d_2 in the second frame, and detection d_2 best matches detection d_1 in the first frame. This way we obtain a subset of matching pairs, such that each detection is matched to exactly one or no detection in the next frame.

To increase the robustness of the matches, a threshold θ_1 was chosen, such that only cell detection pairs whose linking probability was higher than that threshold could be linked.

I have an idea to add additional constraint to prevent linking cells if more than 2 cells are very similar between each other

The affinity function V is learned using a supervised machine learning algorithm, which learns to solve the binary classification problem of linking (or not linking) a pair of cell descriptors. The model is learned by comparing the appearance feature vectors of the detections as well as their positions, which are obtained from the cell detection module.

To finish this section I need to train a model with more data and decide whether to use NB or ANN. Then I need to describe the selected method.

The machine learning algorithm was trained with annotated datasets. The annotations contained the position of cells in the images and links

to matching cells in consecutive images. To train a linking model, cell appearance feature vectors had to be obtained for the dot-annotated cells. First, the cell detection module was trained to detect cells in a dataset. Second, the detector found a set of cell detections, which were matched to the corresponding real annotations. A detection was matched to an annotated cell if and only if the position difference was below a small threshold (10 pixels). This step was required to obtain the cell descriptors of the dot-annotated cells. Finally, the data to train the classifier were constructed as follows. Positive examples were selected as consecutive (linked) cells within each tracklet. Negative examples were chosen from all possible combinations of cells from different tracklets.

Based on the pairs of symmetric matches between cell detections, the system is able to generate a set of robust tracklets \mathbf{T}^{robust} . Cell detections that were not linked to any other cell are also considered robust tracklets, and are included in \mathbf{T}^{robust} for possible further linking in the further steps of the algorithm.

4.3 Global data association DRAFT I

The problem of linking robust tracklets together to form trajectories is formulated as a MAP problem [6] [7] [8]. We first present the formulation, and then in the next section we provide the linear programming implementation.

The data association problem is solved iteratively. Each iteration takes the tracklets obtained in the previous one and does further association. In each iteration ever larger gaps between tracklets are closed.

Given the robust tracklet set \mathbf{T}^{robust} , we maximize the posteriori probability to find the best data association:

Make sure to update this if I decide not to make it iterative, but build a classifier for each possible displacement - which I could weight by the actual distance

Rewrite: This only needs to be in the implementation section

$$\begin{aligned}
\mathbf{T}^* &= \arg \max_{\mathbf{T}} P(\mathbf{T} | \mathbf{T}^{robust}) \\
&= \arg \max_{\mathbf{T}} P(\mathbf{T}^{robust} | \mathbf{T}) P(\mathbf{T}).
\end{aligned}$$

Assuming that the likelihood probabilities of the robust tracklets are conditionally independent given \mathbf{T} , and $T_k \in \mathbf{T}$ cannot overlap with each other, i.e. $\forall T_i, T_j \in \mathbf{T}, i \neq j, T_i \cap T_j = \emptyset$:

$$\mathbf{T}^* = \arg \max_{\mathbf{T}} \prod_{T_i \in \mathbf{T}^{robust}} P(T_i | \mathbf{T}) \prod_{T_k \in \mathbf{T}} P(T_k).$$

Further iterations of the process use the optimal hypothesis set \mathbf{T}^* as input, and perform further association by linking tracklets that are further apart.

The likelihood of a robust tracklet is defined as:

$$P(T_i | \mathbf{T}) = \begin{cases} P_{TP}(T_i) & \text{if } \exists T_k \in \mathbf{T}, T_i \in T_k \\ P_{FP}(T_i) & \text{if } \forall T_k \in \mathbf{T}, T_i \notin T_k \end{cases},$$

Rewrite: This only needs to be in the implementation section

where $P_{TP}(T_i)$ is the probability of T_i being a true positive and $P_{FP}(T_i)$ the probability of T_i being a false positive.

The probability of a tracklet $P(T_k)$ is modelled as a sequence of observations with the Markov property, namely that, given the current observation, the previous and future observations are independent:

$$\begin{aligned}
P(T_k) &= P(\{T_{k_1}, T_{k_2}, T_{k_3}, \dots, T_{k_n}\}), \text{ where } T_{k_i} \in \mathbf{T}^{robust} \\
&= P_{init}(T_{k_1}) P_{link}(T_{k_2} | T_{k_1}) P_{link}(T_{k_3} | T_{k_2}) \dots P_{link}(T_{k_n} | T_{k_{n-1}}) P_{term}(T_{k_n}) \\
&= P_{init}(T_{k_1}) \left[\prod_{j=1:n-1} P_{link}(T_{k_{j+1}} | T_{k_j}) \right] P_{term}(T_{k_n}),
\end{aligned}$$

where $P_{init}(T_{k_1})$ is the probability of T_{k_1} being the first robust tracklet

in T_k , $P_{term}(T_{k_n})$ the probability of T_{k_n} being the last robust tracklet in the sequence, and $P_{link}(T_{k_{j+1}}|T_{k_j})$ transition or linking probabilities for $T_{k_{j+1}}$ and T_{k_j} . The definitions of these terms will be provided in section 4.6.

Note that the MAP problems takes into consideration the possibility of false cell detections, which makes the model ideal for very noisy and low quality microscopic image sequences where the cell detector is likely to find a number of false detections. Additionally, in the analysed image sequences there are often gaps of several frames where the image becomes out of focus and the cells disappear from the field of view. The linking probabilities permit an efficient closing of these gaps.

The benefit of the global data association approach to cell tracking is that it makes a global decision based on the probabilities defined over all the frames of the image sequence rather than propagating the results from frame to frame. This makes the algorithm more robust to errors in the cell detection module.

4.4 Implementation using linear programming DRAFT I

The MAP problem is converted to an integer optimization problem and solved by linear programming.

Let N be the number of input robust tracklets. Let L be a vector containing the likelihoods of all possible hypothesis: initialization, termination, false positive, and linking hypothesis between two robust tracklets. The formulation of these likelihoods is given in section 4.5, and the implementation details in section 4.6.

We also define a matrix H of dimensions $|L| \times 2N$ containing constraints to avoid selecting conflicting hypothesis. Let i represent the index of each new hypothesis and j and index over the columns of H . Then, for a robust tracklet T_k and candidate linking tracklet T_l the entries of matrix H are defined as follows for each possible hypothesis:

$$C_{ij} = \begin{cases} 1 & \text{for an initialization hypothesis if } j = N + k \\ 1 & \text{for a termination hypothesis if } j = k \\ 1 & \text{for a false positive hypothesis if } j = N + k \text{ or } j = k \\ 1 & \text{for a linking hypothesis if } j = k \text{ or } j = N + l \\ 0 & \text{otherwise.} \end{cases}$$

Once the constraint matrix H and likelihood vector L are defined, the original MAP problem from section 4.3 can be solved by selecting a subset of rows from H such that the sum of the corresponding likelihoods in L is maximized, under the non-overlap constraint of tracklets. The MAP problem can be reformulated as a binary linear problem:

$$I^* = \arg \max_I L^T I, \text{ subject to } H^T I = 1,$$

where I is a binary vector containing 1 for the selected rows of the matrix H and 0 elsewhere. The constraint $H^T I = 1$ guarantees that each robust tracklet appears in only one tracklet, or is discarded as a false positive.

For each tracklet an initialization, a termination and a false positive hypothesis is computed. The linking hypothesis is computed for pairs of tracklets where the gap between the tail of the first and head of the next tracklet is shorter than a user specified number of frames.

Add an example H, L and I for illustration

4.5 Hypotheses likelihood definitions

DRAFT I

In this section we define how the different hypothesis are computed. In section 4.6 we will discuss the implementation details.

Due to errors in the cell detection module, all tracklets are candidates

for being false positives. The false positive hypothesis likelihood is *false positive hypothesis* computed as:

$$L_i = \log P_{FP}(T_k).$$

The linking hypothesis measures the likelihood of connecting two *linking hypothesis* tracklets. Candidate tracklet pairs for linking are those for which the distance between the last detection (the tail) of the first tracklet (X_{k_n}) and the first detection (the head) on the second tracklet (X_{l_1}) is less than a specified number of frames. The likelihood of the linking hypothesis is computed as:

$$L_i = \log P_{link}(T_l|T_k) + \frac{\log P_{TP}(T_k) + \log P_{TP}(T_l)}{2}.$$

[6] dealt with cell tracking on image sequences where cell detections could be reliably detected. The authors considered tracklets close to the boundaries of the field of view as candidate for initial tracklets. This work is based on image sequences that were not acquired *in vitro*, but in three dimensional space, in which cells can sink into the background and reappear at any time. The initialization hypothesis indicates the likelihood that a tracklet is the first tracklet in a trajectory. Taking this into consideration new trajectories can be initialized anywhere within the field of view. The corresponding likelihood is computed as:

Make sure this is right

initialization hypothesis

$$L_i = \log P_{init}(T_k) + \frac{\log P_{TP}(T_k)}{2}.$$

Similarly to the initialization hypothesis a cell can sink into the background or leave the field of view. This is taken into account in the termination hypothesis, which is also evaluated for all tracklets. *termination hypothesis* The termination likelihood is computed based on the probability of the tracklet being at the end of a sequences:

$$L_i = \log P_{term}(T_k) + \frac{\log P_{TP}(T_k)}{2}.$$

A true positive tracklet appears in exactly two of initialization,

termination or linking hypothesis. For this reason the likelihood of a tracklet being true positive $\log P_{TP}(T_k)$ is divided into two halves that are included in these hypothesis.

4.6 Computing the likelihoods DRAFT I

In this section we describe the implementation details of the likelihoods: $P_{TP}(T_k)$, $P_{FP}(T_k)$, $P_{init}(T_k)$ and $P_{term}(T_k)$. The likelihoods are directly connected to the input observations and are estimated from training data.

The true and false positive likelihood DRAFT I

The true and false positive likelihoods of a tracklet T_k are defined in terms of the miss detection rate of the cell detector module α , and the number of the cell observations composing the tracklet which we denote $|T_k|$:

$$P_{FP}(T_k) = \pi_{FP} \alpha^{\frac{|T_k|}{\lambda_1}}$$

$$P_{TP}(T_k) = 1 - P_{FP}(T_k),$$

where λ_1 is empirically set to 2, and π_{FP} is a free parameter used to increase or decrease the likelihood that a tracklet is false positive.

The linking hypothesis DRAFT I

The linking hypothesis is computed between pairs of tracklets where the distance (number of frames) between the tail of the first and the head of the second tracklet is less than a threshold. Because of the variable contrast, and poor quality of the imaging technique the measure is computed by taking into account several spatio-temporal and visual features. The different features are outlined in section 4.7. The likelihood of linking tracklet T_l with T_k is:

$$P_{link}(T_l|T_k) = \begin{cases} \pi_{link} V(T_l, T_k) & \text{if } t_{l,1} - t_{k,n} \leq \lambda_2 \\ 0 & \text{otherwise,} \end{cases}$$

where $t_{l,n}$ is the frame index of the last detection of tracklet T_l , $t_{k,1}$ is the frame index of the first detection of tracklet T_k , λ_2 is a threshold indicating the maximum allowed gap for linking two tracklets, $V(.)$ a function that returns the probability that the tracklets should be linked, and π_{link} a free parameter used to increase or decrease the linking likelihood.

The function $V(.)$ is a model incorporating appearance and spatio-temporal features of the candidate linking tracklets. It is trained using an artificial neural network (ANN) with the number of inputs equal to the number of features and a single output that returns a value between 0 and 1.

The binary ANN is trained using annotated image sequences. Positive examples are taken as all combinations of cell detections within each tracklet, and negative the combinations of cell detection pairs of different tracklets. One of the features used in the classifier is the appearance vector, which is obtained for each cell annotation using the cell detection module.

The data used to train the classifier contains features of pairs of tracklets that can be separated by a different number of frames, from 1 to λ_2 . The consequence of using of a binary classifier is that it might return a larger probability of linking two tracklets that are further apart than two tracklets that are closer together. For example, an original trajectory could be detected as three robust tracklets, that have to be linked. The classifier might return a larger likelihood of linking the first and third tracklet than the first and second tracklet. The data association module would then likely link the first tracklet to the third, leaving the second one as a new short trajectory. To overcome this problem the process of linking tracklets is performed iteratively, closing ever larger gaps between tracklets. This way the described problem

Finalize the description of the ANN when I settle on a final shape once I train it using all the data

can no longer occur. A positive side effect of performing the process iteratively is a reduced peak memory usage because of the lower number of hypothesis that are evaluated in each step.

The benefits of this machine learning approach for computing the likelihood of linking two tracklets are twofold. First, it works well on noisy datasets because it uses a large number of features to train the model. Secondly, the large number of features makes it less reliable on accurate cell segmentations in the cell detection module.

Make sure to update this if i decide to build a classifier for each gap length

Remember to update if I decide to build a classifier for each gap size closure

The initialization likelihood DRAFT I

The initialization likelihood is a measure of a tracklet being the first tracklet of a trajectory. This work is based on image sequences with high noise and contrast variance, where cell detections cannot be reliably detected over the entire trajectories of the cells. Additionally, since the images were not acquired *in vitro*, but in three dimensional space, cells can sink into or surface from the background at any time. We take into consideration so that new trajectories can be initialized anywhere within the field of view. The initialization hypothesis is based on the linking hypothesis. It is equal to the likelihood of tracklet T_k not being linked to the most likely linking tracklet in the λ_2 frames *before* its first cell detection:

Make sure this is right

$$P_{init}(T_k) = \begin{cases} \pi_{init}(1 - \max P_{link}(T_k|T_l)) & \forall T_l \in \mathbf{T}, t_{k,1} - t_{l,n} \leq \lambda_2 \\ 0 & \text{otherwise,} \end{cases}$$

where π_{init} is a free parameter that scales the initialization likelihood.

Try looking back only the number of frames you are trying to close... no further, since those could be linked later.

The termination hypothesis DRAFT I

The termination hypothesis measures the likelihood of a tracklet being the last tracklet of a trajectory. It is defined similarly to the initialization hypothesis: the likelihood of tracklet T_k not being linked to the most likely linking tracklet in the λ_2 frames *after* its last cell detection:

$$P_{term}(T_k) = \begin{cases} \pi_{term}(1 - \max P_{link}(T_l|T_k)) & \forall T_l \in \mathbf{T}, t_{l,1} - t_{k,n} \leq \lambda_2 \\ 0 & \text{otherwise,} \end{cases}$$

where π_{term} is a free parameter that scales the termination likelihood.

The scaling parameters DRAFT I

Each of the hypothesis likelihood can be scaled by an appropriate parameter π_{FP} , π_{link} , π_{init} or π_{term} . The setup of these parameters allows a direct manipulation of the linking hypothesis. For example, increasing π_{init} or π_{term} relative to π_{link} makes the system more conservative in linking tracklets. The added benefit of these scaling parameter is that they allow the reuse of the trained classifier for somewhat different datasets, without the need to annotate them and retrain the classifier.

4.7 Features for the linking classifier

OUTLINE

In this section we present an overview of the visual and spatio-temporal features implemented and tested for the classifier for linking tracklets. In section 4.7.3 we enumerate which of these features have been selected to be used in the final classifier.

Cell feature descriptor The difference of vectors containing appearance features obtained from the cell detection module for each

candidate linking tracklet. A description of these features is available in. _____

reference the list of features in the cell detection module

Gap size The number of frames between the tail and head of a pair of tracklets.

Position distance A two dimensional vector containing the absolute distance between the head and tail of a pair of tracklets corresponding to the x and y coordinates.

Square of position distance Same as *Position distance*, but the value is squared.

Distance between points The euclidean distance between the positions of the head and tail of linking tracklets. This is similar to the previous features, but combines the distance between both coordinates into a single value.

Direction angle The difference between the tracklet orientations computed from the last few frames of the first tracklet and the first few frames on the second tracklet. The number of frames used to compute the direction is parametrized.

Orientation variance Similar to the previous feature, but computes the difference of variance of orientation change within tracklets.

Mean displacement The difference of mean displacement between cell detections within the tracklets.

Displacement variance Similar to the previous feature, but computes the difference of variances of displacement between cell detections.

Distance from edge The difference between minimal and maximal distances of the head or tail of the tracklets from the edge of the field of view.

Gaussian broadening distribution This feature is detailed in section 4.7.2.

Augment this list as more features are added

4.7.1 Estimating the velocity with Kalman filters

NEW

This feature has not yet been implemented

4.7.2 Gaussian broadening feature DRAFT I

This section describes a feature that is based on the observation of the motion of the trajectories. It makes sense that the probability of linking two tracklets is inversely proportional to the distance (number of frames) between tracklets. Additionally we can observe that a cell will not travel in a perfectly straight line, but might deviate from it. Using these observations, we have devised a feature inspired by Doppler broadening ¹.

After a tracklet ends, its motion is extrapolated for a number of frames. The probability of a tracklet being at that point along the extrapolated tracklet is assumed to be normally distributed with a mean at the chosen point and a variance. Because of the observation that a tracklet might deviate from its temporary direction, the variance is assumed to be larger at each next extrapolated location. If we place such normal distributions along the extrapolated trajectory, and we normalize their value such that the sum of all the normal distributions is equal to one we obtain a new distribution that describes the probability of a tracklet's position in the future.

We can use this tracklet's distribution to evaluate the likelihood that a candidate tracklet should be linked to it by summing the values of the distribution at the locations corresponding to the cell detection of the new tracklet.

Figure 4.3 shows an example profile of such a distribution, together with two candidate tracklets. The sum of values from the distribution at the location of the tracklet's cell detections indicates that the black tracklet is more likely to be linked to the red one than the green tracklet.

¹http://en.wikipedia.org/wiki/Doppler_broadening

The figure also shows that the distribution correctly adapts to tracklets composed of a single cell detection, or similarly to tracklets with very little movement.

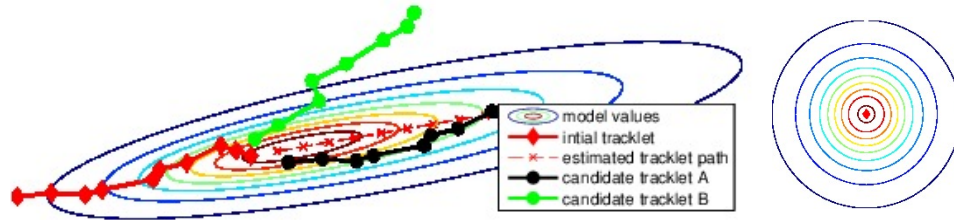


Figure 4.3: Gaussian broadening feature. The distribution is computed for the red tracklet. The contour colours of the distribution are red for higher values and blue as the value decreases. The candidate black tracklet is given a linking likelihood of 0.20, while the green, which is angled from the direction of the red tracklet, a value of only 0.06. On the plot on the right we see that if a tracklet is composed of only one cell detection the value of the feature is equal all around it.

4.7.3 Best feature selection NEW

Define how the best features have been selected

Describe which features performed best

This feature has not yet been implemented

5 Quantitative measurements of cell behaviour NEW

List and explain what features we are interested in, why, and how they are computed.

The paper “Tracking of cell population to understand their spatio-temporal behaviour in response to physical stimuli” presents a comprehensive set of measures.

This feature has not yet been implemented

6 Data acquisition and annotation NEW

6.0.4 Cell culture conditions and imaging modality

NEW

rewrite about the type of cells I am tracking briefly, and focus a lot on the imaging technique. Provide examples of different images from different datasets, illustrate the problem of out of focus, the out-of-sync shutter, etc.

A technique that had crucial impact on the identification of the multistep cascade enabling neutrophil recruitment into inflamed tissues was intravital microscopy. This method allows the visualization of cells in vivo.

More recently, the introduction of microscopes allowing for thicker tissue penetration and higher resolution (spinning-disc and two-photon microscopes), more complex tissues and organs, such as the skin, liver, brain and lung, can also be imaged. The observation of the lung was a challenge for a long time owing to motion artefacts.

The introduction of fluorescence (confocal) microscopy in combination with spinning-disc and two-photon microscopes has allowed the use of fluorescent antibodies for labelling different cell populations on anatomical structures, as well as the use of transgenic mice with fluorescent leukocyte subsets.

TODO: I need more data on the different labeled cells (red, green)
TODO: I need more data on the exact technique and apparatus used to take the images (camera, etc)

6.0.5 The annotation tool NEW

some notes on the importance of accurate annotation, its advantages and disadvantages of dot annotations.

Describe the requirements of an efficient cell annotation tool, such as multipreview, linking, zooming, correct interpretation and saving of the dataformat

An overview of the annotation GUI

the multiple displays filter tools for adding/deleting dots and links
simultaneous display of detections and links

6.0.6 Annotating cell images NEW

What follows is a description of the process of image annotation for use in the machine learning algorithm to detect cells. The image annotation, as required by Arteta's [4] algorithm, are dots on each cell of the image. The algorithm uses these dots as positive examples, and all the remaining pixels as negative examples of a cell.

Rewrite: This describes annotation using Fiji, which was only used at the beginning

We have annotated a subset of frames on the Lung dataset provided by Dr. Leo Carlin. The entire dataset is composed of 150 frames, and is divided into two channels, one for each type of cell (.). We have marked 10 cropped frames on each channel (frame 1, 14, 25, 46, 81, 115, 131, 143 and 150) of dimensions about 128×118 pixels.

I need to learn more about the types of cells I am tracking

The annotation was performed using a Fiji [9] tool called PointPicker [10] which is accessible from *Analyse/Tools/PointPicker*. The annotation is done by manually clicking on each identified cell. The tool outputs a *txt* file containing *x* and *y* coordinates of each annotation, the image number, as well as some other metadata that is not important for us.

It must be noted that the images are very noisy, and it is often hard to distinguish cells from non cells. Figure 6.1 displays an example of an image that was annotated. It is therefore questionable how accurately the learning method will be able to learn the idea of a cell, given that the annotations are far from perfect. It would have been much easier

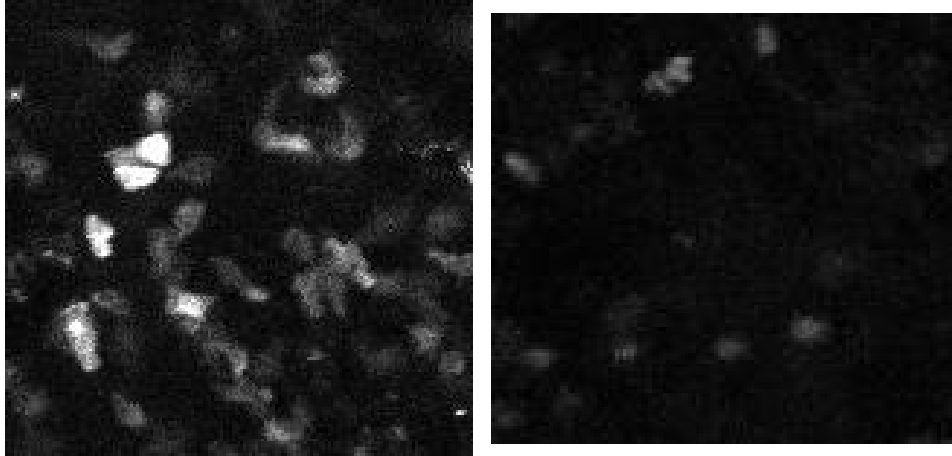


Figure 6.1: Examples of a cropped frame that was annotated for the cell detection machine learning algorithm. Each frame belongs to a different channel of the dataset.

to perform the learning using a synthetic dataset.

The data is then loaded into MATLAB and converted into the format required by the algorithm. The data tidying is performed by the script *prepareTrainData.m*.

7 Experimental results NEW

Think about which experiments to do, analyses, comparison with other methods if possible

This feature has not yet been implemented

7.1 Cell detector NEW

Figure 7.1 displays a temporal view of the detected cells. The vertical axis represents the frame of the sequence. The figure clearly shows that “cell tracks” are clearly discernible, even if the number of outliers is significant. For the tracking module it is better to have a higher recall than precision, as outliers can be much more easily discarded than segmented tracks linked.

7.1.1 Performance NEW

Measure the speed of detection in images of different sizes, and different number of cells

7.1.2 Detection accuracy NEW

7.2 Cell tracker NEW

Define the different measures of accuracy

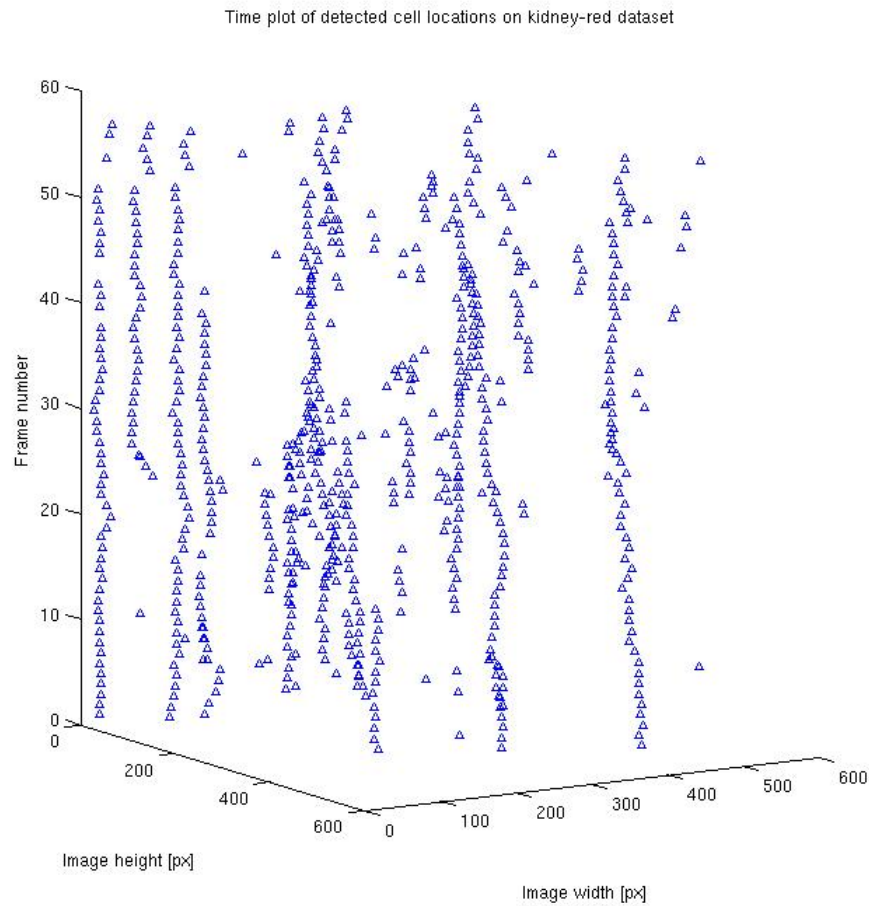


Figure 7.1: Cells detected over 60 consecutive frames are visualized as a time series. The vertical axis corresponds to the frames. Even in this raw detection data, it is possible to see the tracks of some of these cells.

7.2.1 Performance metrics NEW

7.2.2 Performance NEW

Measure the speed of generating tracks, as a measure of per 1, 100, 1000 frames, depending on the number of tracks

7.2.3 Tracking accuracy

8 Discussion and conclusion

NEW

Write the conclusion

8.1 Future work NEW

Define what other things could be worked on: mitosis, statbilization, image clearing process, skipping bad frames

Bibliography

- [1] P. K. Elzbieta Kolaczowska, “Neutrophil recruitment and function in health and inflammation,” 2013.
- [2] J. Pillay, I. den Braber, N. Vrisekoop, L. M. Kwast, R. J. de Boer, J. A. M. Borghans, K. Tesselaar, and L. Koenderman, “In vivo labeling with 2h2o reveals a human neutrophil lifespan of 5.4 days,” *Blood*, vol. 116, no. 4, pp. 625–627, 2010.
- [3] P. S. Tofts, T. Chevassut, M. Cutajar, N. G. Dowell, and A. M. Peters, “Doubts concerning the recently reported human neutrophil lifespan of 5.4 days,” *Blood*, vol. 117, no. 22, pp. 6050–6052, 2011.
- [4] C. Arteta, V. Lempitsky, J. A. Noble, and A. Zisserman, “Learning to detect cells using non-extremal regions,” in *Proceedings of the 15th International Conference on Medical Image Computing and Computer-Assisted Intervention - Volume Part I, MICCAI’12*, (Berlin, Heidelberg), pp. 348–356, Springer-Verlag, 2012. 9, 13, 35
- [5] R. Bise, T. Kanade, Z. Yin, and S. il Huh, “Automatic cell tracking applied to analysis of cell migration in wound healing assay,” in *Engineering in Medicine and Biology Society, EMBC, 2011 Annual International Conference of the IEEE*, pp. 6174–6179, Aug 2011. 18
- [6] R. Bise, Z. Yin, and T. Kanade, “Reliable cell tracking by global data association,” in *ISBI*, pp. 1004–1010, IEEE, 2011. 21, 25
- [7] L. Zhang, Y. Li, and R. Nevatia, “Global data association for multi-object tracking using network flows,” in *Computer Vision*

- and Pattern Recognition, 2008. CVPR 2008. IEEE Conference on*, pp. 1–8, June 2008. 21
- [8] C. Huang, B. Wu, and R. Nevatia, “Robust object tracking by hierarchical association of detection responses,” in *Computer Vision - ECCV 2008* (D. Forsyth, P. Torr, and A. Zisserman, eds.), vol. 5303 of *Lecture Notes in Computer Science*, pp. 788–801, Springer Berlin Heidelberg, 2008. 21
- [9] J. Schindelin, I. Arganda-Carreras, E. Frise, V. Kaynig, M. Longair, T. Pietzsch, S. Preibisch, C. Rueden, S. Saalfeld, B. Schmid, J.-Y. Tinevez, D. J. White, V. Hartenstein, K. Eliceiri, P. Tomancak, and A. Cardona, “Fiji: an open-source platform for biological-image analysis,” *Nature Methods*, vol. 9(7), pp. 676–682, 2012. 35
- [10] S. F. I. o. T. L. Philippe Thévenaz, Biomedical Imaging Group, “Point picker: An interactive imagej plugin that allows storage and retrieval of a collection of landmarks,” May 2014. 35